

# Design of Microwave Wide-Band Quadrature Hybrid Using Planar Transformer Coupling Method

Wei-Shin Tung, Hsu-Hsiang Wu, and Yi-Chyun Chiang, *Member, IEEE*

**Abstract**—A lumped-element quadrature hybrid consisting of two-section inductive coupled  $\pi$ -networks is presented. A synthesizing method involving a new set of design equations are also developed to realize the proposed hybrid with very good balance in both magnitude and phase between the output ports over a 38% fractional bandwidth. The measurements of the two prototypes show quite good agreement with the theoretical predictions. The proposed hybrid is compact and suited to be implemented by conventional microwave-integrated-circuit technology.

**Index Terms**—Microwave integrated circuit (MIC), planar quadrature hybrid.

## I. INTRODUCTION

IN VARIOUS microwave circuits, such as balance amplifiers, image rejection mixers, and phase shifters, quadrature hybrids are used to achieve the desired circuit characteristics. The most commonly used microwave quadrature hybrids are the branch-line Langer couplers, which consist of four or several coupled quarter-wavelength lines [1], [2]. At the lower microwave frequency bands, the quarter-wavelength lines constructed on a conventional microwave integrated circuit (MIC) or a monolithic microwave integrated circuit (MMIC) occupy too much valuable chip area. Thus, various lumped-element quadrature hybrids are proposed for using in MIC or MMIC applications [3]–[7]. The generalized method of synthesizing lumped- and lumped-distributed-element directional couplers in co-directional, contra-directional, and trans-directional configurations was first proposed by Vogel [4]. Recently, we proposed a design method for realizing a two-section co-directional lumped-element hybrid with wide-band characteristics [5]. Other than the capacitive coupling mechanism employed in the above papers, Ali and Podell proposed a contra-directional transformer-coupled hybrid, which shows a very wide-band characteristic [6]. In this paper, we propose a new hybrid design, which consists of two-section transformer-coupled  $\pi$ -networks connected by a single inductor ( $L_m$ ) in the center, as shown in Fig. 1. This hybrid features fewer components than the previous conventional configurations. A new set of design equations are also proposed to realize the hybrid with good magnitude and phase balances at the output ports and at the same time, an operation bandwidth only slightly less than conventional ones is achieved.

Manuscript received November 20, 2002; revised February 27, 2003. This work was supported by the National Science Council, Taiwan, R.O.C., under Contract NSC91-2219-E-182-003.

The authors are with the Institute of Electronics Engineering, Chang-Gung University, Taiwan, R.O.C. (e-mail: d9028105@stmail.cgu.edu.tw; elemarkwu@pchome.com.tw; ycchiang@mail.cgu.edu.tw).

Digital Object Identifier 10.1109/TMTT.2003.814311

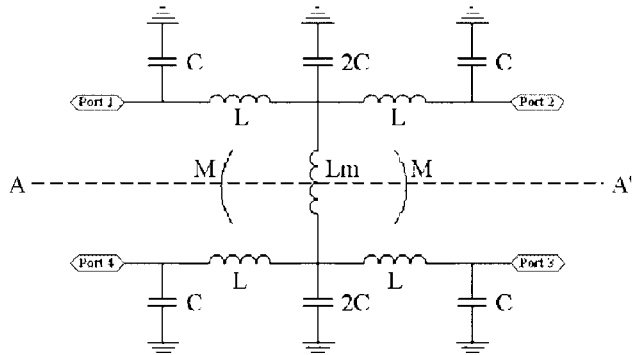


Fig. 1. Lumped quadrature hybrid realized by two-sectional  $\pi$ -network with transformer-coupling feature.

The proposed design equations take the phase relationship, denoted by  $\theta_A$ , between ports 1 and 2, as shown in Fig. 1, into consideration to calculate the values of the elements in Fig. 1. Since  $\theta_A$  is introduced as an extra unknown in the hybrid design procedure, values of the elements of the hybrid can be obtained according to the given  $\theta_A$ . A conventional microwave circuit simulator is then applied to evaluate the performance of the hybrids and find the optimal values of the elements. Applying the proposed synthesizing method, we found two sets of element values realizing the hybrid with very good magnitude and phase balances between the output ports, as well as achieving input matching over a 38% fractional bandwidth.

Two prototypes operating at UHF and S-bands are designed and fabricated to verify the design concept. On-board elements and conventional surface-mount technology (SMT) devices are also used to realize the prototype circuit on a conventional FR4 printed circuit board (PCB) substrate. The measured results of the hybrid prototypes are very close to the theoretic predictions. The proposed hybrid is also suited to be implemented by other commercial multilayer technologies, such as low-temperature co-fired ceramic (LTCC) or MMIC to further reduce the size of the hybrid circuit.

## II. DESIGN OF PLANAR TRANSFORMER-COUPLED LUMPED QUADRATURE HYBRID PROTOTYPE

The circuit of the transformer-coupled lumped hybrid in Fig. 1 is symmetrical about the  $AA'$ -plane and all ports of hybrid are assumed to be terminated at impedance  $Z_0$ . It can, therefore, be analyzed by the conventional even- and odd-mode analysis method. The transmission wave matrix of the even- and odd-mode half-circuits is given by

$$[T_{e,o}] = \begin{bmatrix} T_{11e,o} & T_{12e,o} \\ T_{21e,o} & T_{22e,o} \end{bmatrix}$$

and the elements in this transmission matrix are

$$T_{11e} = 1 + 2Y\Lambda_e(2 + Y\Lambda_e) + j \cdot (1 + Y\Lambda_e) \times \left[ \frac{\Lambda_e}{j} Y_0 + \frac{Y}{j} Z_0(2 + Y\Lambda_e) \right] \quad (1.1a)$$

$$T_{11o} = 1 + 2\Lambda_o [2Y + Y_m + Y\Lambda_o(Y + Y_m)] + j \cdot \left\{ \frac{\Lambda_o}{j} Y_0 [1 + \Lambda_o(Y + Y_m)] + Z_0(1 + Y\Lambda_o) \times \frac{[2Y + Y_m + Y\Lambda_o(Y + Y_m)]}{j} \right\} \quad (1.1b)$$

$$T_{12e} = j \cdot (1 + Y\Lambda_e) \cdot \left[ -\frac{\Lambda_e}{j} Y_0 + \frac{Y}{j} Z_0(2 + Y\Lambda_e) \right] \quad (1.2a)$$

$$T_{12o} = j \cdot \left\{ -\frac{\Lambda_o}{j} Y_0 [1 + \Lambda_o(Y + Y_m)] + Z_0(1 + Y\Lambda_o) \times \frac{[2Y + Y_m + Y\Lambda_o(Y + Y_m)]}{j} \right\} \quad (1.2b)$$

$$T_{12e,o} = -T_{21e,o} \quad (1.3)$$

$$T_{22e} = 1 + 2Y\Lambda_e(2 + Y\Lambda_e) - j \cdot (1 + Y\Lambda_e) \times \left[ \frac{\Lambda_e}{j} Y_0 + \frac{Y}{j} Z_0(2 + Y\Lambda_e) \right] \quad (1.4a)$$

$$T_{22o} = 1 + 2\Lambda_o [2Y + Y_m + Y\Lambda_o(Y + Y_m)] - j \cdot \left\{ \frac{\Lambda_o}{j} Y_0 [1 + \Lambda_o(Y + Y_m)] + Z_0(1 + Y\Lambda_o) \times \frac{[2Y + Y_m + Y\Lambda_o(Y + Y_m)]}{j} \right\} \quad (1.4b)$$

where  $Y_0$ ,  $Y_m$ , and  $Y$  represent the admittance of  $Z_0$ ,  $L_m$ , and  $C$  in Fig. 1, respectively;  $\Lambda_e$  and  $\Lambda_o$  are equivalent to  $j\omega(L + M)$  and  $j\omega(L - M)$ , respectively. According to the method of synthesis proposed in [4], the following conditions must be satisfied for constructing a co-directional ( $S_{41} = 0$ ) quadrature coupler:

$$T_{12e} = T_{12o} = 0 \quad (2)$$

$$|T_{11e}|^2 = |T_{11o}|^2 = 1. \quad (3)$$

Substituting (2) into (1.2a) yields the following conditions for the even-mode half circuit:

$$1 + \Lambda_e Y = 0 \quad (4a)$$

or

$$\Lambda_e Y = Y Z_0(2 + \Lambda_e Y) \quad (4b)$$

and the other equation, corresponding to the odd-mode half circuit obtained from (2) and (1.2b) is

$$\Lambda_o Y_0 [1 + \Lambda_o(Y + Y_m)] = Z_0(1 + Y\Lambda_o) \times [2Y + Y_m + Y\Lambda_o(Y + Y_m)]. \quad (5)$$

Equations (4) and (5) are now substituted into (1.1a) and (1.1b) for the even- and odd-mode half-circuit, respectively, and the following equations for  $T_{11e,o}$  as functions of circuit elements are obtained:

$$T_{11e} = -1 \quad (6a)$$

or

$$T_{11e} = 1 + 2(\Lambda_e Y_0)^2 + j \cdot 2 \left( \frac{\Lambda_e}{j} \right) Y_0(1 + \Lambda_e Y) \quad (6b)$$

and

$$T_{11o} = 1 + 2\Lambda_o(2Y + Y_m) + 2(Y + Y_m)Y\Lambda_o^2 + j \cdot \left( \frac{Y_0}{j} \right) [2\Lambda_o + 2\Lambda_o^2(Y + Y_m)]. \quad (7)$$

Considering the magnitude and phase relationships between  $S_{21}$  and  $S_{31}$  of a 3-dB co-directional coupler, a generalized form of  $T_{11e}$  and  $T_{11o}$  is proposed here as follows:

$$T_{11e} = \frac{1}{\sqrt{2}}(\cos \theta_A + \sin \theta_A) - j \frac{1}{\sqrt{2}}(\sin \theta_A - \cos \theta_A) \quad (8)$$

$$T_{11o} = \frac{1}{\sqrt{2}}(\cos \theta_A - \sin \theta_A) - j \frac{1}{\sqrt{2}}(\sin \theta_A + \cos \theta_A) \quad (9)$$

where  $\theta_A$  is the phase of  $S_{21}$ . Equating (6a) and (6b) to (8), it yields two different situations. The first situation is derived from equating (6a) to (8) to obtain the value of  $\theta_A$  to be  $5\pi/4$ . Equating (7) to (9) and substituting the obtained value of  $\theta_A$  into (9) then yields the following two equations:

$$1 + 2\Lambda_o(2Y + Y_m) + 2(Y + Y_m)Y\Lambda_o^2 = 0 \quad (10)$$

$$\left( \frac{Y_0}{j} \right) [2\Lambda_o + 2\Lambda_o^2(Y + Y_m)] = 1. \quad (11)$$

Based on (4a), (5), (10), and (11), the values of  $Y_m$ ,  $Y$ ,  $\Lambda_e$ , and  $\Lambda_o$  can be obtained as

$$Y = \frac{-(j\Lambda_o + Z_o)}{Z_o\Lambda_o} \quad (12)$$

$$Y_m = \frac{j(2Y_o\Lambda_o^2 + Z_o)}{2\Lambda_o^2} \quad (13)$$

and

$$\Lambda_e = \frac{Z_o\Lambda_o}{(j\Lambda_o + Z_o)} \quad (14)$$

where  $\Lambda_o$  is a positive pure imaginary number and its absolute value must be less than  $Z_0/\sqrt{2}$  to keep  $Y_m$  negative. Mathematical analytic software (such as MatLab) is used to solve the previous equations, and a microwave circuit simulator (such as Ansoft Serenade) is used to evaluate the performance of hybrid constructed by the values of the elements obtained above. Table I lists eight sets of 2.4-GHz hybrid elements' values and their performances corresponding to various values of  $\Lambda_o$ . Column 5 of Table I shows a fractional bandwidth for which the return loss (RL) of input port greater than 15 dB and the associated magnitude imbalance and phase difference between the output ports are listed in columns 6 and 7, respectively. It is shown the hybrid constructed by elements listed in row 4 of Table I demonstrates the most wide-band characteristic, while we desire the hybrid performance in the design band having less than 15-dB RL and phase difference and magnitude imbalance less than  $5^\circ$  and 1 dB, respectively. Fig. 2 presents the simulated characteristics of the hybrid consisting of ideal lumped elements with the values shown in row 4 of Table I. As it shown, the hybrid demonstrates quite good characteristics at a frequency range from  $0.8f_0$  to  $1.2f_0$ . The third-order harmonic rejection between port 1 and the other ports ( $S_{21}$ ,  $S_{31}$ , and  $S_{41}$ ) of the hybrid are all greater than 30 dB. Therefore, the proposed

TABLE I

PERFORMANCE AND ELEMENTS' VALUES FOR CONSTRUCTING 2.4-GHz QUADRATURE HYBRID DERIVED FROM THE FIRST SITUATION, OF WHICH  $T_{11e} = -1$  AND  $\theta_A = 5\pi/4$  ARE ASSUMED

$\Lambda_o$	L (nH)	M (nH)	C (pF)	L <sub>m</sub> (nH)	Fractional Bandwidth (RL > 15dB)	Magnitude Imbalance (dB)	Phase Difference (degree)
35j	5.029	2.708	0.568	162.470	21.25%	3.4	90±2.1
30j	3.482	1.492	0.884	8.526	57.50%	3.5	90±1.9
25j	2.487	0.829	1.326	3.316	52.08%	3.5	90±1.1
19j	1.646	0.386	2.164	1.346	38.33%	1.0	90±1.7
15j	1.208	0.213	3.095	0.728	18.75%	0.3	90±1.5
10j	0.746	0.083	5.305	0.288	9.17%	0.3	90±1.6
5j	0.350	0.018	11.937	0.068	3.75%	0.5	90±1.6
2j	0.135	0.003	31.831	0.011	1.25%	0.4	90±1.9

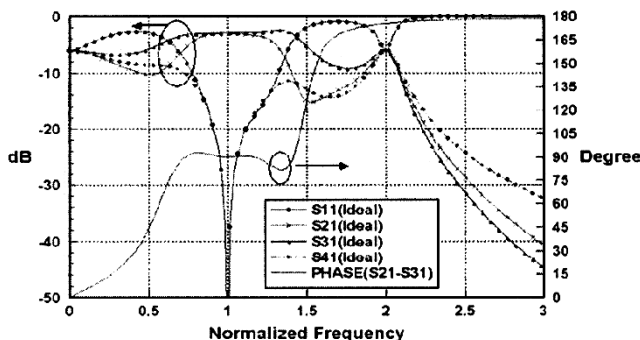


Fig. 2. Simulated S-parameters of the transformer-coupled lumped quadrature hybrid constructed by ideal lumped elements.

hybrid structure also can provide a low-pass filtering function for using in some microwave mixer or amplifier designs.

The second situation is derived from equating (6b) to (8), and (7) to (9). Equations (4b) and (5) are also taken into consideration. The following equations are obtained to calculate the elements' values:

$$1+2(\Lambda_e Y_o)^2 = \frac{1}{\sqrt{2}} \cos \theta_A + \frac{1}{\sqrt{2}} \sin \theta_A \quad (15)$$

$$1+2\Lambda_o(2Y+Y_m) + 2(Y+Y_m)Y\Lambda_o^2 = \frac{1}{\sqrt{2}} \cos \theta_A - \frac{1}{\sqrt{2}} \sin \theta_A \quad (16)$$

$$2\left(\frac{\Lambda_e}{j}\right) Y_o(1+\Lambda_e Y) = -\left(\frac{1}{\sqrt{2}} \sin \theta_A - \frac{1}{\sqrt{2}} \cos \theta_A\right) \quad (17)$$

and

$$\left(\frac{Y_o}{j}\right) [2\Lambda_o + 2\Lambda_o^2(Y+Y_m)] = -\left(\frac{1}{\sqrt{2}} \sin \theta_A + \frac{1}{\sqrt{2}} \cos \theta_A\right). \quad (18)$$

Obviously, five unknowns must be determined from the above four equations. Hence, the values of elements shown in Fig. 1 can be derived for an arbitrary given value of  $\theta_A$ . Using the software mentioned above, the elements' values and characteristics of the proposed hybrid can be obtained for various values of  $\theta_A$ . Table II lists eight sets of elements' values and their performances according to various values of  $\theta_A$ . It is shown that the hybrid constructed by elements in row 7 is most promising for wide-band application.

TABLE II

PERFORMANCE AND ELEMENTS' VALUES FOR CONSTRUCTING 2.4-GHz QUADRATURE HYBRID DERIVED FROM THE SECOND SITUATION, OF WHICH  $\theta_A$  IS ARBITRARY

$\theta_A$	L (nH)	M (nH)	C (pF)	L <sub>m</sub> (nH)	Fractional Bandwidth (RL > 15dB)	Magnitude Imbalance (dB)	Phase Difference (degree)
150°	2.083	0.548	2.690	7.028	7.92%	2.0	90±1.8
180°	2.400	0.664	1.983	3.790	12.08%	3.3	90±1.3
210°	2.513	0.775	1.512	3.349	19.17%	2.9	90±0.8
225°	2.487	0.830	1.3260	3.316	41.67%	3.5	90±1.1
240°	2.405	0.883	1.161	3.349	38.33%	6.1	90±1.6
270°	2.069	0.994	0.889	3.490	36.67%	9.3	90±5.5
300°	1.520	1.110	0.657	3.811	42.92%	1.1	90±1.8
315°	1.172	1.172	0.550	3.995	40.00%	0.7	90±2.1

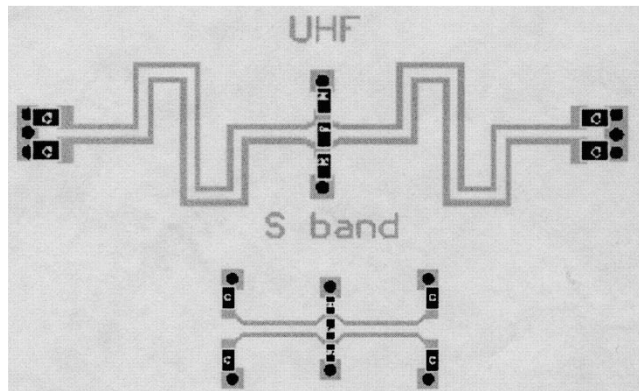


Fig. 3. Physical layout of proposed lumped hybrids consisting of on-board lumped elements and SMT devices.

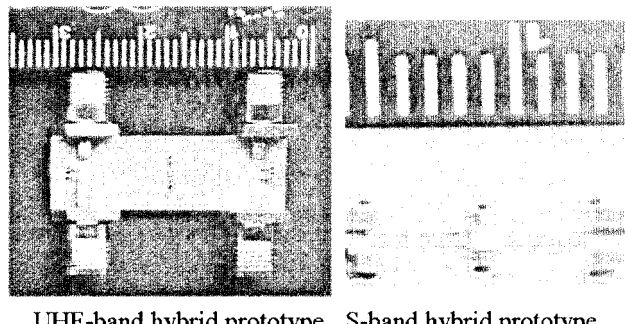


Fig. 4. Photographs of UHF- and S-band lumped hybrid prototypes.

### III. DESIGN AND MEASUREMENT OF QUADRATURE HYBRID PROTOTYPE

To verify the proposed design concept, quadrature hybrid prototypes operated at the *S*-band and UHF band are designed and fabricated on conventional FR4 PCB substrates, of which the relative dielectric constant is 4.3, the thickness is 0.8 mm, and the metal thickness is 17.5  $\mu$ m. The hybrid performances in Table I and II reveal that the hybrid constructed by the element listed in row 7 of Table II yield the most promised characteristics. However, the operation bandwidth of the hybrid in row 4 of Table I is only a few percent less than the most promised one, but the request of the 0.386-nH mutual inductor of the hybrid is much less than that in Table II, and should be easily implemented by using conventional PCB technology. The parallel-coupled microstrip and meander line on the FR4 substrate

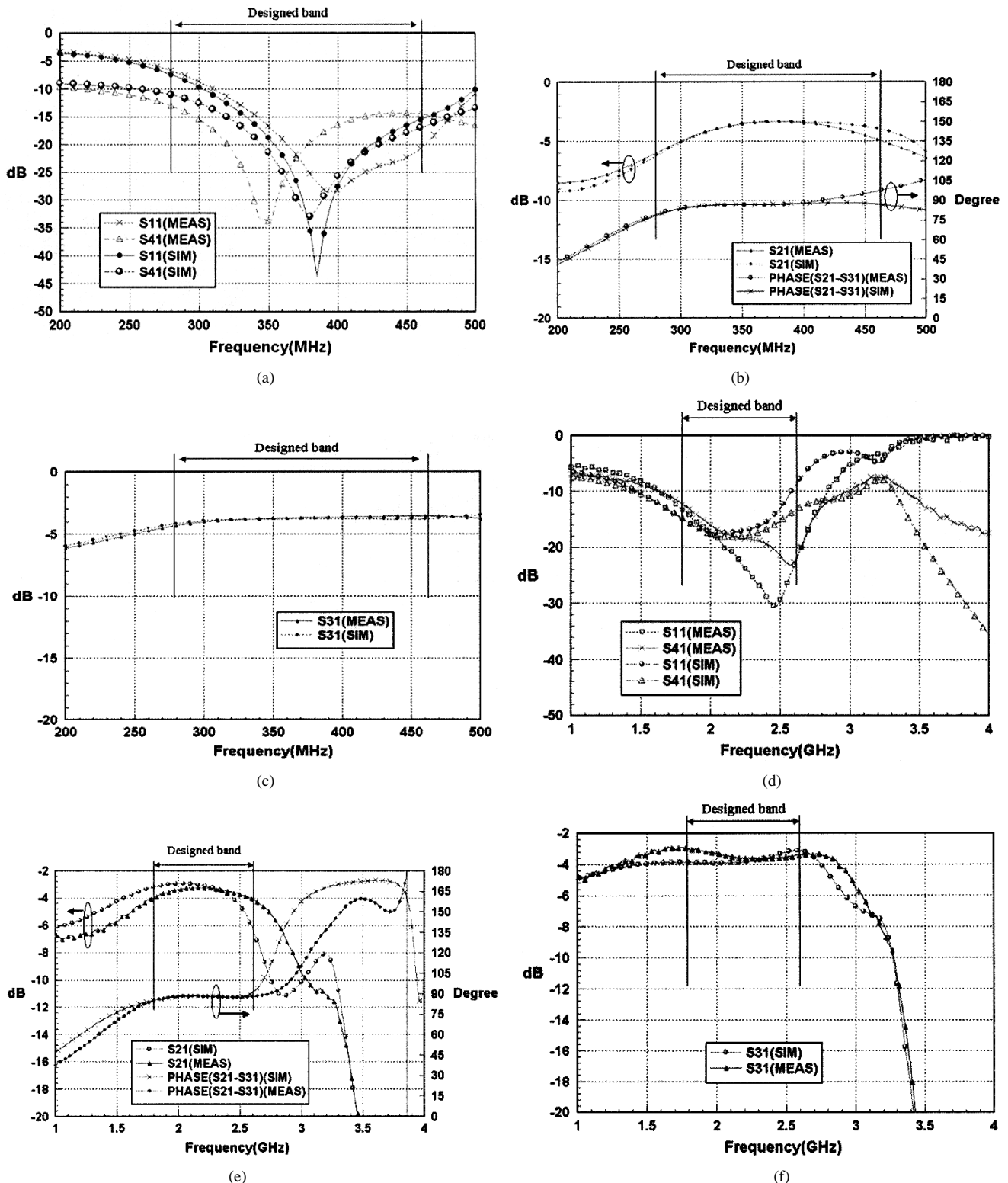


Fig. 5. (a) Measured and simulated  $S_{11}$  and  $S_{41}$  of the UHF-band hybrid. (b) Measured and simulated  $S_{21}$  and phase difference between ports 2 and 3 of the UHF-band hybrid. (c) Measured and simulated  $S_{31}$  of the UHF-band hybrid prototype. (d) Measured and simulated  $S_{11}$  and  $S_{41}$  of the S-band lumped hybrid. (e) Measured and simulated  $S_{21}$  and phase difference between ports 2 and 3 of the S-band hybrid. (f) Measured and simulated  $S_{31}$  of the S-band hybrid.

are adopted to realize the inductive-coupled inductors. Other lumped elements in the prototypes are realized by commercial SMT devices. Fig. 3 depicts the PCB layouts of the prototypes. To realize the on-board elements, a commercial electromagnetic (EM) simulator was adopted to analyze various physical ge-

ometries, shown in Fig. 3, and determine the proper geometries for realizing the proposed hybrids. Other elements of the coupler prototypes, such as shunt capacitors ( $C$  and  $2C$ ) and central coupling inductor ( $L_m$ ) are implemented by using commercial surface-mount devices whose elements' values are close to

ideal. The characteristics of the prototypes are obtained by cascading the simulated  $S$ -parameters of on-board elements and the SMT devices'  $S$ -parameters provided by the devices' manufacturers. The simulated magnitude of the insertion losses is approximately 1.0 dB lower than that realized by ideal elements because the metal and dielectric losses occur in the PCB substrate. However, the imbalance of the magnitude between the direct and coupled ports is still less than 1 dB; the difference of the phases between the direct and coupled ports is also kept less than 5° over 38% bandwidth, which is slightly less than that realized by the ideal elements. Fig. 4 shows the photographs of quadrature hybrid prototypes that are fabricated on PCB substrates. The sizes of the  $S$ - and UHF-band prototypes are 1 cm  $\times$  0.4 cm and 2.4 cm  $\times$  1 cm, respectively.

The measured results of the prototypes are obtained by connecting two of the four ports of the hybrid circuit to an HP8753D network analyzer through coaxial cables and by connecting a subminiature type-A (SMA) launcher or an MIC test fixture to the other two ports, terminated with  $50\ \Omega$ . The conventional thru-reflect-line (TRL) calibration technique is used to shift the measuring reference planes from the SMA launchers to the input ports of the prototypes. To show the difference of the measurements and theoretical predictions, the measured results and theoretical predictions are superimposed in Fig. 5(a)–(f).  $S_{11}$  and  $S_{41}$  represent the reflect line (RL) of the input port and the isolation between the input and isolation ports, respectively.  $S_{21}$  and  $S_{31}$  represent the insertion losses of the direct and coupled ports of the hybrid, respectively. As it is shown, some unknown parasitic elements in the practical circuit result in some disagreement between the measured and simulated results. However, the measurements are close to the theoretical predictions and it shows quite good magnitude and phase balances in the design bands. Although these measured bandwidths are slightly less than the conventional hybrid reported in [5], the proposed hybrid consists of fewer lumped components and provides better high-frequency rejection than the conventional lumped hybrid.

#### IV. CONCLUSION

The design of a wide-band planar quadrature hybrid constructed by a planar transformer has been presented. Using the mutual inductance of a transformer to achieve the requested coupling between microstrip inductors can decrease the number of elements to realize the hybrid; it can also provide better high-frequency rejection between input and output ports. The prototype circuits are designed and fabricated to verify the proposed design concept. The measured results are very close to the theoretical predictions and the measured operating bandwidth, which shows very good magnitude and phase balances, as well as input RL, is over a 38% fractional bandwidth. Conventional multilayer technology, such as LTCC or MMIC technologies, can enable the proposed hybrid to be constructed with a smaller size than the presented PCB version.

#### REFERENCES

- [1] D. M. Pozar, *Microwave Engineering*. New York: Wiley, 1998, ch. 8, pp. 379–383.
- [2] J. Lange, "Interdigitated stripline quadrature coupler," *IEEE Trans. Microwave Theory Tech.*, vol. MTT-17, pp. 1150–1151, Dec. 1969.
- [3] R. K. Gupta and W. J. Getsinger, "Quasilumped element 3- and 4-port networks for MIC and MMIC applications," in *IEEE MTT-S Int. Microwave Symp. Dig.*, San Francisco, CA, 1984, pp. 409–411.
- [4] R. W. Vogel, "Analysis and design of lumped- and lumped-distributed-element directional couplers for MIC and MMIC applications," *IEEE Trans. Microwave Theory Tech.*, vol. 40, pp. 253–262, Feb. 1992.
- [5] Y. C. Chiang and C. Y. Chen, "Design of a wide-band lumped-element 3-dB quadrature coupler," *IEEE Trans. Microwave Theory Tech.*, vol. 49, pp. 476–479, Mar. 2001.
- [6] F. Ali and A. Podell, "Design and applications of a 3 : 1 bandwidth GaAs monolithic spiral quadrature hybrid," in *IEEE GaAs Integrated Circuits Symp. Dig.*, New Orleans, LA, Oct. 1990, pp. 279–282.
- [7] J. Hogerheiden, M. Ciminera, and G. Jue, "Improved planar spiral transformer theory applied to a miniature lumped element quadrature hybrid," *IEEE Trans. Microwave Theory Tech.*, vol. 45, pp. 543–545, Apr. 1997.



**Wei-Shin Tung** was born in Taichung, Taiwan, R.O.C., in 1977. He received the B.S. degree in electrical engineering from the Tatung University, Taipei, Taiwan, R.O.C., in 1999, the M.S. degree in electrical engineering from the Chang-Gung University, Tao Yuan, Taiwan, R.O.C., in 2001, and is currently working toward the Ph.D. degree in electronics engineering at Chang-Gung University.

He is currently involved with the development of the multiplayer embedded RF circuit modules.



**Hsu-Hsiang Wu** was born in Kaohsiung, Taiwan, R.O.C., in 1981. He received the B.S. degree in electronics engineering from the Chang-Gung University, Tao Yuan, Taiwan, R.O.C., in 2003.

He is currently a compulsory serviceman. His research interests include RF design and MIC design.



**Yi-Chyun Chiang** (S'87–M'91) received the B.S. degree in marine technology, and the M.S. and Ph.D. degrees in electronics engineering from the Chiao Tung University, Hsin Chu, Taiwan, R.O.C., in 1982, 1987, and 1992, respectively.

He is currently an Associate Professor with the Department of Electronics Engineering, Chang-Gung University, Tao Yuan, Taiwan, R.O.C. His main research interests are the area of developing GaAs MMICs for the applications in personal wireless communication and characterization of linear and nonlinear RF models of the submicrometer Si CMOS transistors.